Canted magnetic structure arising from rare-earth mixing in the Laves-phase compound $(Nd_{0.5}Tb_{0.5})Co_2$

Y. G. Xiao,[1] Q. Huang,[2] Z. W. Ouyang,[1] F. W. Wang,[1] J. W. Lynn,[2] J. K. Liang,[1,3] and G. H. Rao[1,*]

[1]*Beijing National Laboratory for Condensed Matter Physics, Institute of Physics, Chinese Academy of Sciences, Beijing 100080, People's Republic of China*

[2]*NIST Center for Neutron Research, National Institute of Standards and Technology, Gaithersburg, Maryland 20899-8562, USA*

[3]*International Center for Materials Physics, Academia Sinica, Shenyang 110015, People's Republic of China*

The crystal and magnetic structures of Laves-phase compound $(Nd_{0.5}Tb_{0.5})Co_2$ have been investigated by high resolution neutron powder diffraction at different temperatures. Magnetization measurement and neutron diffraction reveal two magnetic transitions at $T_C \approx 173$ K and $T_M \approx 47$ K, respectively. At room temperature, the compound crystallizes in the $MgCu_2$-type (C15) structure. Below T_C, rhombohedral distortion and large anisotropic magnetostriction take place and persist down to 4 K. In contrast to the binary rare earth (R)-Co Laves-phases RCo_2, a noncollinear magnetic structure (canted) is deduced for $(Nd_{0.5}Tb_{0.5})Co_2$, based on the Rietveld refinement of the neutron diffraction data at 50 K and 4 K. In addition, the correlation between lattice distortion and easy magnetization direction (EMD) commonly observed for binary RCo_2 is violated in $(Nd_{0.5}Tb_{0.5})Co_2$. Though the crystal structure remains rhombohedral, the EMD of the R sublattice is close to the [110] direction at 50 K of the pseudocubic lattice and along the [111] direction at 4 K, respectively. The difference of the canting angle between the magnetic structures at 50 K and 4 K is small, indicating stable canted configurations. The lattice parameters exhibit a discontinuity around T_M, suggesting a first-order transition between the two canted magnetic structures. The dilution of magnetic anisotropy of the R sublattice and the contribution of the magnetic anisotropy of the Co sublattice are responsible for the observations.

PACS number(s): 75.25.+z, 75.30.Kz, 75.50.−y

I. INTRODUCTION

Metamagnetic compounds, which undergo field-induced magnetic phase transitions, are potential novel materials for industry and technology applications, because the field-induced magnetic transition is frequently accompanied by giant magnetocaloric effect, large magnetostriction, and giant magnetoresistance, etc.[1–3] For more than 20 years, rare earth (R) Laves-phases RCo_2 have been an interesting subject in condensed matter physics and for the study of band metamagnetism, owing to their simple magnetic and crystallographic structures for verifying different physical models.[4]

RCo_2 crystallizes in the $MgCu_2$-type structure (Laves C15 phase, space group $Fd\bar{3}m$). For nonmagnetic rare earths such as Y and Lu, the RCo_2 is nonmagnetic but shows characteristic features of exchange enhanced paramagnetism. Ferromagnetism in YCo_2 and $LuCo_2$ can be induced by applying a magnetic field higher than a critical field of about 70 T.[5] It means the d-electron subsystem exhibits a magnetic instability, which can be interpreted by the nearly fulfilled Stoner criterion for ferromagnetism of the density of states (DOS) at the Fermi level of the compounds.[6] Thermally induced fluctuating magnetic moments have been predicted by the theory.[7] The spin fluctuation scenario is indispensable for understanding the dynamic physical properties of the RCo_2 compounds. For magnetic rare earths, the molecular field exerted on the Co sublattice by the R sublattice could be larger than the critical field and induce the magnetism of Co sublattice.

One of the important physical properties interesting to applications is the larger anisotropic magnetostriction exhibited by RCo_2 below the Curie temperature T_C.[4,8] The large magnetostriction results in various lattice distortions of the cubic RCo_2 via strong magnetoelastic interaction. For binary RCo_2, a close correlation between the easy magnetization direction (EMD) and the crystallographic symmetry of the distorted Laves phase has been observed, i.e., a rhombohedral distortion corresponds to the EMD of [111] of the pseudocubic structure, a tetragonal distortion to the EMD of [100], and an orthorhombic distortion to the EMD of [110] (Ref. 9). Based on the special symmetry of the rare-earth site in the C15 structure, Cullen and Clark elucidated the relationship between the spontaneous anisotropic magnetostriction, which is determined by the EMD, and the structural distortions in the Laves-phase cubic compounds RT_2 (T = Fe, Co, Ni).[10]

Considering the hybridization effect between $5d$ and $3d$ states, it is usually observed that for rare-earth transition metal intermetallic compounds, the $4f$-$3d$ spin-spin coupling is antiferromagnetic, leading to a parallel alignment of $3d$ and $4f$ moments in the light lanthanide compounds ($J = |L-S|$) and to an antiparallel alignment in the heavy lanthanide compounds ($J = L+S$). All binary RCo_2 compounds seem to follow this universal picture.[4,8] Therefore, for the heavy rare-earth RCo_2, the moment of the R sublattice (M_R) and that of the Co sublattice (M_{Co}) couples antiferromagnetically. In this case, if the anisotropy of the Co sublattice is comparable to that of the R sublattice or the difference of sublattice magnetization, $|M_R - M_{Co}|$, is reduced, a noncollinear magnetic structure, i.e., a canted magnetic structure, could become stable. The noncollinear magnetic structure can provide important information of the f-d coupling. A

partial dilution of the magnetic R sublattice by nonmagnetic yttrium or lutetium can decrease the difference $|M_R - M_{Co}|$, but at the same time it reduces the molecular field exerting on the Co atoms and may destabilize the magnetism of the Co sublattice in RCo_2. Brommer *et al.* investigated the non-collinear magnetic structure and the f-d interaction in $Lu_{1-x}Tm_y(Co_{0.98}Al_{0.12})_2$.[11] The partial substitution of Al for Co is to stabilize the magnetism of the Co sublattice. Swift and Wallace studied the magnetic characteristics of mixed Laves-phase compounds $(R', R'')Al_2$.[12] In order to interpret the composition dependence of the saturation magnetization of $(R', R'')Al_2$, they proposed that the spins of R' and R'' couple ferromagnetically and therefore the moments of R' and R'' align parallel if both are light or both are heavy rare earths and antiparallel if one is a light rare earth and the other is a heavy rare earth. Using this model, Ouyang *et al.* elucidated the composition dependence of the saturation magnetization of the mixed compounds $(Nd_{1-x}Tb_x)Co_2$ satisfactorily.[13] These studies imply that a mixing of light and heavy rare earths in RCo_2 will reduce the magnetization of the R sublattice, whereas the molecular field exerted on the Co sublattice by the light and heavy rare-earth metals will be in the same direction and additive, retaining the magnetism of the Co sublattice. This could be an effective way to study the canted magnetic structure and the f-d interaction in RCo_2 and to enhance our understanding of the physics of RCo_2 compounds. Unfortunately, oriented investigation on the light-heavy rare-earths mixed RCo_2 has not yet achieved a deserved attention.

Neutron powder diffraction reveals that $NdCo_2$ undergoes a tetragonal distortion around $T_C \approx 100$ K and an orthorhombic distortion at $T \approx 42$ K,[14] while $TbCo_2$ exhibits a rhombohedral distortion below $T_C \approx 240$ K.[15] The collinear magnetic structure models with the expected EMD, i.e., along [001] direction of the pseudocubic lattice for the tetragonal distortion, [110] for the orthorhombic distortion, and [111] for the rhombohedral distortion, fitted the neutron diffraction data satisfactorily. At the lowest temperature investigated, $M_R = 2.8\mu_B$/f.u., $M_{Co} = 1.46\mu_B$/f.u. for $NdCo_2$ (9 K), and $M_R = 8.3\mu_B$/f.u., $M_{Co} = 2.44\mu_B$/f.u. for $TbCo_2$ (14 K). Assuming a ferromagnetic $4f$-$4f$ spin coupling, an antiferromagnetic $4f$-$3d$ spin coupling, and a collinear magnetic structure, it is easy to estimate that $M_R = 2.75\mu_B$/f.u. and $M_{Co} = 1.95\mu_B$/f.u. for the equiatomically mixed compound $(Nd_{0.5}Tb_{0.5})Co_2$. Taking into consideration of the reduced $|M_R - M_{Co}|$, the different EMDs and different lattice distortions of $NdCo_2$ and $TbCo_2$, it is particularly intriguing to study the magnetic structure, lattice distortion, and its correlation with the EMD of the mixed compound $(Nd_{0.5}Tb_{0.5})Co_2$.

II. EXPERIMENTAL

A polycrystalline sample of $(Nd_{0.5}Tb_{0.5})Co_2$ was prepared by arc melting the constituent elements with a purity of 99.9% in an atmosphere of high-purity argon as described in Refs. 14 and 15. The weight loss during arc melting was less than 0.1 wt. %. The ingots were annealed at 800 °C under vacuum for 14 days. X-ray powder diffraction analysis con-
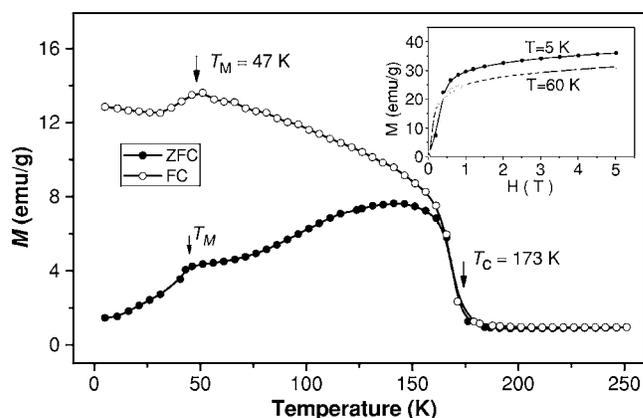

FIG. 1. Temperature dependence of magnetization of $(Nd_{0.5}Tb_{0.5})Co_2$ in a field of 0.05 T. The inset shows the field dependence of magnetization at 5 K and 60 K.

firmed that the compound crystallized in the cubic Laves-phase C15 structure at room temperature.[13]

Magnetizations of the compound as functions of temperature and applied field were measured on a superconducting quantum interference device magnetometer (SQUID) under a field of 0.05 T and in fields up to 5 T, respectively.

Neutron powder diffraction (NPD) experiments were performed at the NIST Center for Neutron Research (NCNR). The magnetic order parameter was determined on the BT-7 spectrometer with a neutron wavelength of 2.4649 Å provided by a pyrolytic graphite monochromator and filter. NPD data for refinement of the crystal and the magnetic structures were collected on the high-resolution, 32-counter BT-1 diffractometer. A Cu (311) monochromator was used to produce a monochromatic neutron beam of wavelength 1.5402(1) Å. Collimators with horizontal divergence of 15, 20, and 7 min of arc were used before and after the monochromator and after the sample, respectively. Data were collected in the 2θ range of 10°–160° with a step of 0.05°. The program FULLPROF (Refs. 16 and 17) was used for the Rietveld refinement of the crystal and the magnetic structures of the compound, using the following values of the scattering amplitudes: $b(Nd) = 0.769$, $b(Tb) = 0.738$, and $b(Co) = 0.249$ ($\times 10^{-12}$ cm).

III. RESULTS

A. Magnetization

Figure 1 shows the temperature dependence of magnetization of $(Nd_{0.5}Tb_{0.5})Co_2$ measured in zero-field-cooling-warming (ZFC) and field-cooling-warming (FC) modes, respectively, under a field of 0.05 T. The Curie temperature is derived to be $T_C = 173$ K. A sudden drop of the magnetization occurs at $T_M = 47$ K. The magnetization curve of $(Nd_{0.5}Tb_{0.5})Co_2$ is reminiscent of that of binary $NdCo_2$,[18] which, however, exhibited a jump at $T_M = 42$ K ($< T_C$) on the magnetization curve. Magnetic structure analysis given below reveals that the drop of the magnetization at $T_M = 47$ K corresponds to a spin-reorientation transition in $(Nd_{0.5}Tb_{0.5})Co_2$. Figure 2 shows the temperature dependence
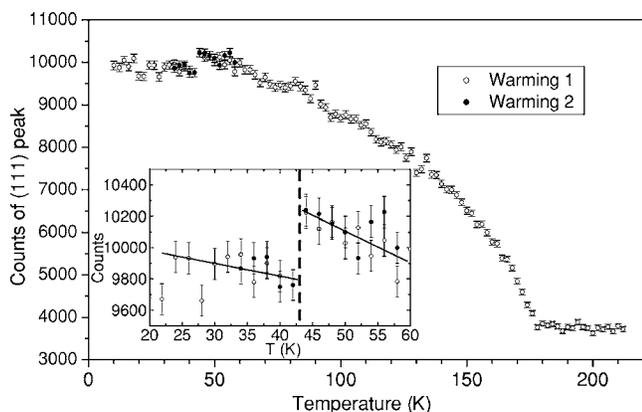
FIG. 2. Temperature dependence of the NPD counts of the (111) peak of the cubic structure. The inset magnifies the region around $T_M = 43$ K.

FIG. 3. Neutron powder diffraction pattern of $(Nd_{0.5}Tb_{0.5})Co_2$ at room temperature. The crosses represent the observed intensities, the solid line is the calculated pattern. The difference between the observed and calculated intensities is shown at the bottom. The vertical bars indicate the expected Bragg reflection positions.

of the NPD counts of (111) peak of the cubic structure measured on the BT-7 diffractometer in a zero-field-cooling-warming mode, which reproduces well the FC magnetization behavior shown in Fig. 1. The difference in magnetization below T_C for the FC and ZFC processes (Fig. 1) can be attributed to magnetic domain-wall pinning effects in bulk sample, which cannot be detected by neutron powder diffraction. The NPD experiment shows that long-range magnetic ordering develops below 177 K and an abrupt drop of the intensity takes place at 43 K.

The field dependence of magnetization at 5 K and 60 K in fields up to 5 T is shown as the inset in Fig. 1. The magnetization increases rapidly below 0.5 T and tends to approach saturation afterwards. Extrapolating M versus $1/H$ curve to $1/H=0$, the saturation magnetizations of $1.89\mu_B/f.u.$ at 5 K and $1.65\mu_B/f.u.$ at 60 K are derived according to the law of approaching saturation.

B. Crystal structure at room temperature

Neutron powder diffraction pattern of $(Nd_{0.5}Tb_{0.5})Co_2$ at room temperature is shown in Fig. 3. The compound crystallizes in the cubic Laves-phase structure (C15, $MgCu_2$-type, space group $Fd\bar{3}m$). No atomic ordering of Nd and Tb was detected. The NPD peaks are attributed to the nuclear scattering at room temperature. The rare-earth atoms occupy the $8a$ sites (1/8, 1/8, 1/8) and the Co atoms occupy the $16d$ sites (1/2, 1/2, 1/2). Rietveld refinement of the crystal structure gives a lattice parameter of $a=7.2560(6)$ Å and isotropic atomic temperature factors of $B(Nd/Tb)=0.33(2)$ Å^2, $B(Co)=0.3(3)$ Å^2 ($R_{wp}=4.3\%$, $\chi^2=1.06$). The lattice parameter derived from NPD is in good agreement with that derived from x-ray powder diffraction.[13]

C. Crystal and magnetic structures below T_C

Both Fig. 1 and Fig. 2 show a sudden change in magnetization around $T_M=47$ K, indicative of a change in crystal structure or/and magnetic structure in $(Nd_{0.5}Tb_{0.5})Co_2$. Neutron powder diffraction patterns of the compound at 50 K ($>T_M$) and 4 K ($<T_M$) are shown in Fig. 4. Below
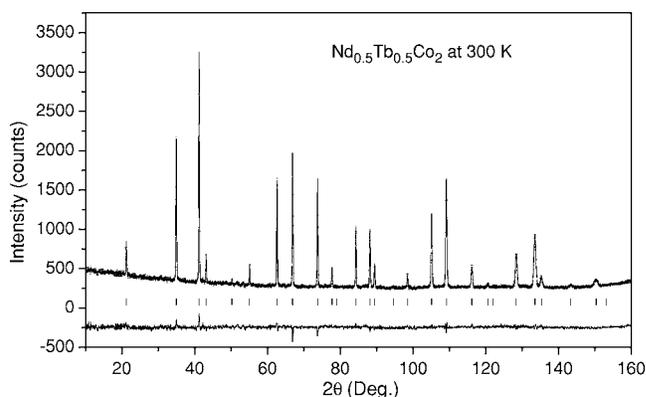
Curie temperature, the crystal structure distorts due to the strong magnetoelastic interaction. Unlike $NdCo_2$, in which the crystal and magnetic structural transitions occurred simultaneously at $T_M=42$ K, the compound $(Nd_{0.5}Tb_{0.5})Co_2$ exhibits a rhombohedral distortion (space group $R\bar{3}m$) below T_C and down to 4 K as revealed by the obvious splitting of the cubic (440) peak into the rhombohedral (208) and (220) peaks (in hexagonal setting) shown in the inset.

For binary Laves-phases RCo_2, a close correlation between the EMD of the compounds and the lattice distortions is generally observed. The character of the unit cell distortion is determined by the orientation of the easy axis of magnetization in all cases.[9] For the rhombohedral distortion of the
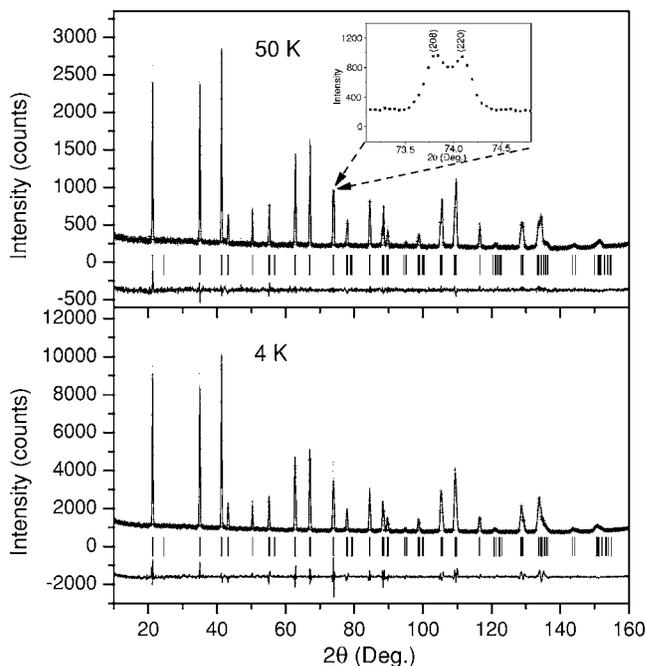

FIG. 4. NPD patterns of $(Nd_{0.5}Tb_{0.5})Co_2$ at 50 K and 4 K. The meaning of the symbols and lines are the same as in Fig. 3. The inset shows the splitting of the cubic (440) peak.

lattice, the EMD is expected to be along the [111] direction. However, using a collinear magnetic structure model with the EMD along the [111] direction of the pseudocubic unit cell, i.e., the [001] direction of the rhombohedral structure in the hexagonal setting, as for $TbCo_2$ compound (magnetic space group $R\bar{3}m'$), Rietveld refinements of the NPD data of $(Nd_{0.5}Tb_{0.5})Co_2$ at 50 K and 4 K gave out much smaller saturation moments than those determined from magnetization measurements ($M_{cal} \sim 0.6\mu_B$/f.u. vs $M_{exp} = 1.89\mu_B$/f.u. at 5 K and $1.65\mu_B$/f.u. at 60 K). We therefore rule out this collinear magnetic structure model for $(Nd_{0.5}Tb_{0.5})Co_2$.

For a cubic lattice, the first magnetocrystalline anisotropy constant K_1 of the rare earth is determined not by the second-order Stevens factor but by the fourth-order Stevens factor β_J (assuming $|K_2| \ll |11K_1|$),[19]

$$K_1 \propto \beta_J J_R (J_R - 1/2)(J_R - 1)(J_R - 3/2)\langle r_{4f}^4 \rangle. \quad (1)$$

Extensive experiments show that the EMD of RCo_2 is along the [111] direction when β_J is positive and along the [100] or the [110] directions when β_J is negative, in good agreement with the prediction of Eq. (1). The fact that a collinear magnetic structure is observed for all RCo_2 indicates a dominant contribution of the R sublattice to the anisotropy of the compounds and a strong f-d coupling.

Since the parent compounds $NdCo_2$ and $TbCo_2$ favor different EMD, [110] for $NdCo_2$ and [111] for $TbCo_2$, in accordance with the prediction of Eq. (1) (β_J is negative for Nd and positive for Tb), the mixing of Nd and Tb is expected to reduce the effective magnetocrystalline anisotropy of the R sublattice. On the other hand, the Co sublattice favors an EMD of [100] direction as observed in $GdCo_2$. In this case, the Co sublattice anisotropy may also make a significant contribution to the EMD of the mixed compound $(Nd_{0.5}Tb_{0.5})Co_2$ and a noncollinear magnetic structure may be stabilized. Lowering the magnetic space group to $R12'/m'$, which is equivalent to the standard $C2'/m'$, magnetic structure models with the moments of all the atoms lying on the mirror plane perpendicular to the a axis of the $R\bar{3}m$ (in hexagonal setting) fit the NPD data of $(Nd_{0.5}Tb_{0.5})Co_2$ at 50 K and 4 K satisfactorily as shown in Fig. 4. The saturation moments derived from the Rietveld refinements, $1.71(12)\mu_B$/f.u. at 50 K and $1.87(19)\mu_B$/f.u. at 4 K, agree well with those derived from magnetization measurements ($1.65\mu_B$/f.u. at 60 K and $1.89\mu_B$/f.u. at 5 K). Since the isotropic temperature factors are small for both the R and Co at 300 K, the temperature factors at 5 K and 50 K are fixed to the values linearly interpolated between those at 300 K and zero at 0 K, i.e., $B(Nd/Tb) = 0.055$ Å^2 and $B(Co) = 0.049$ Å^2 at 50 K, $B(Nd/Tb) = 0.004$ Å^2 and $B(Co) = 0.004$ Å^2 at 4 K, during the refinements; otherwise, the atomic moments and the temperature factors are strongly correlated. The data of crystal and magnetic structures derived from Rietveld refinements for $(Nd_{0.5}Tb_{0.5})Co_2$ at 50 K and 4 K are listed in Table I.

In the crystal structure of RCo_2 with the space group $R\bar{3}m$, the R atoms sit on the 6c sites with symmetry of 3m and one quarter of the Co atoms on the 3b sites with sym-

TABLE I. Data of crystal and magnetic structures derived from Rietveld refinements for $(Nd_{0.5}Tb_{0.5})Co_2$ compound at 50 K and 4 K (space group: $R\bar{3}m$). $R = (Nd_{0.5}Tb_{0.5})$ at 6c (0,0,z), Co1 at 3b (0,0,1/2) and Co2 at 9e (1/2,0,0).

		$T = 50$ K	$T = 4$ K
a (Å)		5.1123(1)	5.1290(2)
c (Å)		12.5832(4)	12.5107(6)
V (Å)		284.81(1)	285.02(2)
R	z	0.1256(2)	0.1260(3)
	$M_a(\mu_B)$	0.92(7)	0.0
	$M_b(\mu_B)$	1.84(13)	0.0
	$M_c(\mu_B)$	2.25(9)	2.64(7)
	Moment(μ_B)	2.75(5)	2.64(7)
Co1	$M_a(\mu_B)$	−0.39(9)	0.0
	$M_b(\mu_B)$	−0.78(17)	0.0
	$M_c(\mu_B)$	−1.30(12)	−1.26(12)
	Moment(μ_B)	1.46(12)	1.26(12)
Co2	$M_a(\mu_B)$	−0.71(4)	−0.64(8)
	$M_b(\mu_B)$	−1.43(8)	−1.29(16)
	$M_c(\mu_B)$	0.0	−0.77(8)
	Moment(μ_B)	1.24(7)	1.35(11)
R_P/R_{wp} (%)		4.51/5.53	4.19/6.30
χ^2		0.852	4.20

metry $\bar{3}m$. Magnetic space groups associated with $R\bar{3}m$ and compatible with a long-range magnetic ordering of these atoms should contain a threefold rotation 3 or $\bar{3}$. However, Rietveld refinement based on such magnetic space groups gave a magnetization of $(Nd_{0.5}Tb_{0.5})Co_2$ much smaller than the experimental one. To construct a reasonable magnetic structure model for the compound, we then considered the maximal nonisomorphic subgroups of $R\bar{3}m$ without the threefold rotation, i.e., $R12/m$ ($C2/m$ in standard notation). For the adopted magnetic space group $R12'/m'$, the R atoms on the 6c sites, Co atoms on the 3b sites, and one third of the Co atoms on the 9e sites (referring to the lattice symmetry $R\bar{3}m$), all have two independent components of the moment: $M_a = M_b/2$, and M_c, while the remaining Co atoms on the 9e sites have three independent components: M_a, M_b, and M_c. Considering the same chemical environment of the Co atoms on the 9e sites, we used a constraint of $M_a = M_b/2$ for all the Co atoms on the 9e sites in the Rietveld refinements. By trial and error, the final results listed in Table I with a few fixed parameters, i.e., $M_c = 0$ for Co2 at 50 K and $M_a = M_b/2 = 0$ for R and Co1 at 4 K, are adopted on the basis of smaller reliability factors of the refinement (R_{wp}, R_p, χ^2), reasonable moments for the atoms and the derived total magnetization of the compound. Therefore, the proposed magnetic structure models for $(Nd_{0.5}Tb_{0.5})Co_2$ at different temperatures make sense in satisfactorily interpreting the NPD patterns and the magnetization data, but they are nevertheless not exclusive.

The proposed magnetic structures of $(Nd_{0.5}Tb_{0.5})Co_2$ are schematically illustrated in Fig. 5. The magnetic structures are not collinear and the EMD deviates away from the [111]
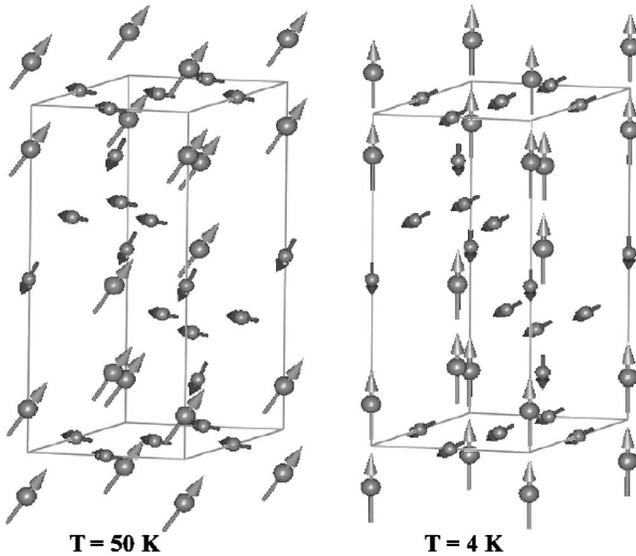
FIG. 5. Illustration of the magnetic structures of $(Nd_{0.5}Tb_{0.5})Co_2$ at 50 K and 4 K. Larger and smaller balls represent rare-earth atoms and Co atoms, respectively.

FIG. 6. Schematic presentation of the magnetic structures of $(Nd_{0.5}Tb_{0.5})Co_2$ at 50 K and 4 K on the mirror plane perpendicular to a axis.

direction of the cubic unit cell, though the crystal structure distorts rhombohedrally. This feature is completely different from that of the binary RCo_2 compounds, i.e., the generally observed correlation between the EMD and the lattice distortion for binary RCo_2 is violated. The derived R moments are $2.75(5)\mu_B$ and $2.64(7)\mu_B$ at 50 K and 4 K, respectively, which are very close to the expected average R moment $(2.75\mu_B)$ within the assumption of ferromagnetic $4f$-$4f$ spin coupling. In addition, the R moment aligns almost along the [110] direction at 50 K and along the [111] direction at 4 K. The R moment forms an angle of $35(4)°$ with the [111] direction at 50 K (the ideal value of the angle between [110] and [111] in a cubic structure is 35.26°).

The proposed magnetic structure models for $(Nd_{0.5}Tb_{0.5})Co_2$ suggest that the Co moments on different crystallographic sites ($3b$ and $9e$) are different, in both magnitude and direction. At 50 K, the moment of Co on the $3b$ sites is $1.5(1)\mu_B$, very close to the atomic moment of metallic Co. However, the average atomic moment of Co is $1.30(6)\mu_B$ (=half the Co-sublattice moment M_{Co}). At 4 K, the Co moments are 1.3(1) and $1.4(1)\mu_B$ for Co on the $3b$ and $9e$ sites, respectively, with an average of $1.33(9)\mu_B$. Extensive studies on RCo_2 compounds show that the average Co moment in the metamagnetic Co sublattice falls in the range of $0.6-1.1\mu_B/Co$.[4] In addition, it seems that the direction of the Co moments on the $3b$ sites always follows antiferromagnetically that of the R moments. The Co moment on the $3b$ sites forms an angle of $173(13)°$ at 50 K and of 180° at 4 K with the R moment, respectively.

The data shown in Table I and magnetic structures shown in Fig. 5 indicate that the Co moments couple antiferromagnetically to the R moments in all three directions. Therefore, within the framework of two-sublattice model, the R sublattice is of heavy rare earth character in $(Nd_{0.5}Tb_{0.5})Co_2$. Figure 6 shows schematically the relative orientations of the R sublattice moment (M_R) and Co-sublattice moment (M_{Co}) at
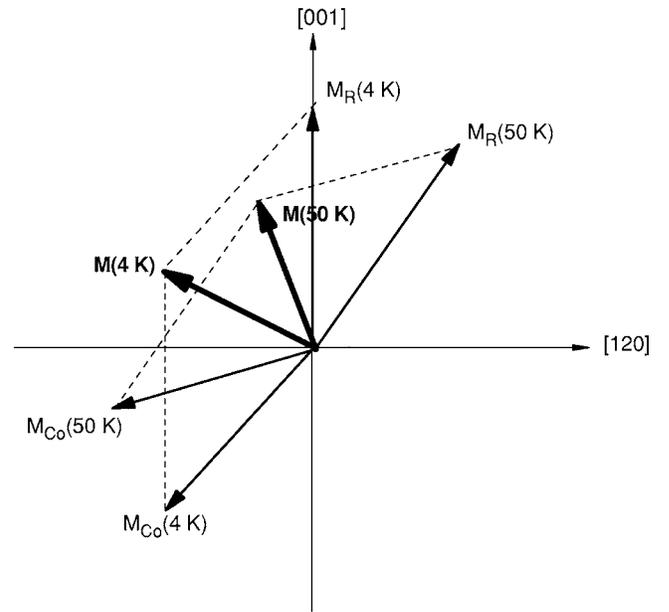
50 K and 4 K on the mirror plane on which the moments lie. The magnitudes of M_R and M_{Co} are comparable. The total moment M of the compound forms an angle of $20(6)°$ with the c axis at 50 K and an angle of $62(6)°$ with the c axis at 4 K, respectively. The moments of the R sublattice and the Co sublattice arrange in a canted form. The canting angles are $141(4)°$ at 50 K and $137(6)°$ at 4 K, respectively. Thus, the transition at $T_M = 47$ K exhibited on the magnetization curve (Fig. 1) can be regarded as a spin-reorientation transition between the two canted magnetic structures.

IV. DISCUSSION

NPD experiments show that the mixed compound $(Nd_{0.5}Tb_{0.5})Co_2$ exhibits a rhombohedral distortion below T_C. Figure 7 manifests the temperature dependence of the splitting of the cubic (533) peak into the rhombohedral peaks $(315/401)$ and $(01\underline{1}1)$ (in hexagonal setting). The variations of 2θ of the $(315/401)$ and $(01\underline{1}1)$ peaks with temperature are shown in Fig. 7(a), from which the lattice parameters a and c are estimated [Fig. 7(b)]. As the temperature decreases, the rhombohedral distortion increases. The lattice parameter c increases obviously, indicating an increase of the magnetostriction constant λ_{111}, whereas the lattice parameter a decreases slightly. A discontinuous change in lattice parameters occurs around 43 K, indicative of a first-order phase transition. As the temperature decreases, the lattice expands for $T_M < T < T_C$ and contracts for $T < T_M$ along the [111] direction of the pseudocubic lattice [Fig. 7(c)]. The lattice expansion and contraction are almost of the same magnitude at T_M. This feature can be associated with the EMD of the compound. As shown in Figs. 5 and 6, the EMD is close to the [111] direction at 50 K, while it is close to the direction perpendicular to the [111] at 4 K. Therefore, the significant
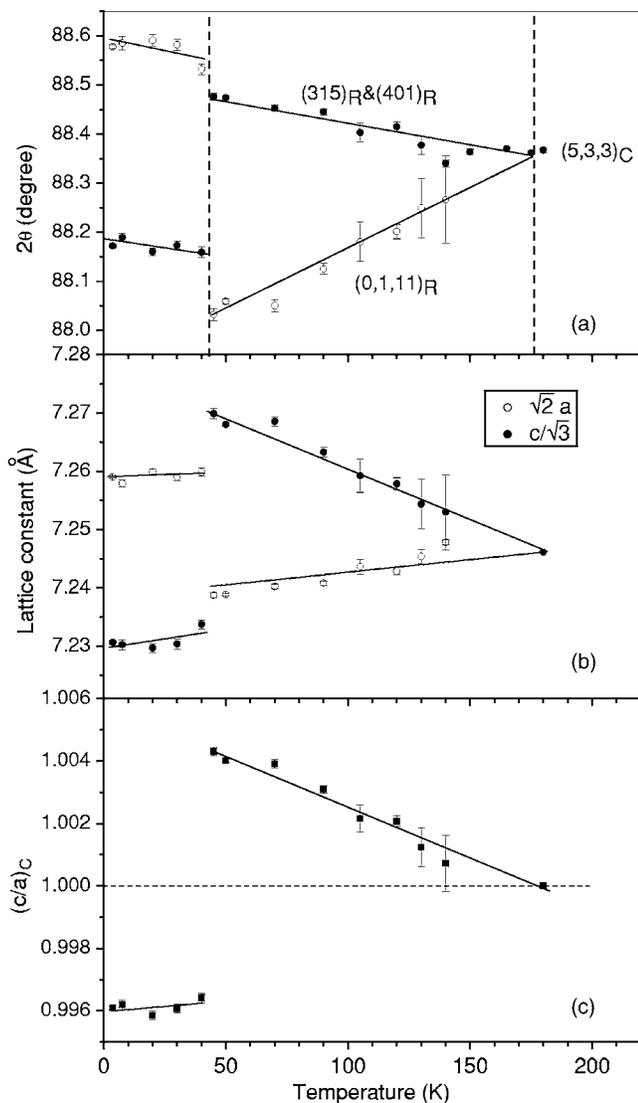
FIG. 7. Temperature dependence of the splitting of the cubic (533) peak into the rhombohedral (315/401) and (01$\bar{1}$1) peaks. (a) 2θ position, (b) estimated lattice parameters, and (c) c/a ratio scaled to cubic lattice $a_C = \sqrt{2}a_R$, $c_C = c_R/\sqrt{3}$.

lattice expansion occurs along the EMD direction of the compound.

In general, the magnetic anisotropy of a rare-earth transition metal intermetallic compound is dominated by that of the rare-earth metal, especially in the low-temperature range, owing to the highly asymmetric $4f$ electron clouds. For binary RCo$_2$ compounds, anisotropy and magnetization of the R sublattice are usually larger than those of the Co sublattice (for heavy rare earth, $M_R > 5\mu_B$/f.u., $M_{Co} < 2\mu_B$/f.u.). In zero field or under fields B smaller than B_C [$= |n_{fd}(M_R - M_{Co})| > 80$ T for heavy rare earth, where n_{fd} is the molecular field coefficient],[12] the compound exhibits a collinear magnetic structure with the EMD coincident with the EMD of the R sublattice due to strong f-d coupling. Therefore, a correlation between the EMD and the type of lattice distortion is usually observed for binary RCo$_2$.[9]

Since NdCo$_2$ and TbCo$_2$ favor different EMD, the mixing of Nd and Tb in (Nd$_{0.5}$Tb$_{0.5}$)Co$_2$ leads to reductions of both

the R-sublattice anisotropy and the difference between sublattice moments $|M_R - M_{Co}|$, supposing a ferromagnetic coupling of the $4f$-$4f$ spins in the R sublattice. Then, the anisotropy of the Co sublattice could become comparable to that of the R sublattice and a canted magnetic structure could be stabilized. Within the two-sublattice model and considering only the first anisotropy constant K_1, the canting angle α, the angle between the R-sublattice moment M_R and the Co-sublattice moment M_{Co}, is determined by[20]

$$\frac{2K_1(R)K_1(Co)}{M_R M_{Co} K} \cos \alpha = n_{fd}, \qquad (2)$$

where $K = \sqrt{K_1(R)^2 + K_1(Co)^2 + 2K_1(R)K_1(Co)\cos 2\alpha}$.

Considering that the Co sublattice favors an EMD along the [100] direction, the anisotropy of R sublattice perpendicular to the [111] direction can be enhanced for the mixed compound (Nd$_{0.5}$Tb$_{0.5}$)Co$_2$, leading to the EMD of the R sublattice close to [110] at 50 K, similar to the EMD in NdCo$_2$. As the temperature decreases, the anisotropy of the R sublattice increases rapidly and dominates at low temperature, the EMD of the R sublattice switches to the [111] direction at 4 K, the same EMD as in TbCo$_2$. At 50 K, the canting angle $\alpha = 141°$, thus $\cos \alpha = -0.777$, $\cos 2\alpha = 0.208$. Since $K_1(R) \gg K_1(Co)$ and $|\cos 2\alpha| < |\cos \alpha|$ at low temperature, the canting angle will not be changed much when the change in EMD occurs at $T_M \approx 47$ K according to Eq. (2), which is consistent with the canting angle of 137(6)° at 4 K derived from NPD data. However, due to the strong magnetoelastic interaction, the lattice parameters are altered abruptly as the spin-reorientation transition takes place.

V. SUMMARY

The mixed compound (Nd$_{0.5}$Tb$_{0.5}$)Co$_2$ crystallizes in the cubic Laves-phase structure (MgCu$_2$-type, space group $Fd\bar{3}m$) at room temperature. Below Curie temperature $T_C (\approx 173$ K), the crystal structure shows a rhombohedral distortion down to 4 K. In contrast to the binary RCo$_2$ compounds with the rhombohedral distortion, the easy magnetization direction (EMD) does not coincide with the cubic [111] direction. Canted magnetic structures are stabilized below T_C, and the moments between the R sublattice and the Co sublattice couple antiferromagnetically in all three directions. A spin-reorientation transition takes place at $T_M \approx 47$ K. Significant lattice expansion occurs along the EMD. The lattice parameters show discontinuous changes at T_M, which indicates the first-order transition character of the spin-reorientation transition. The EMD of the R sublattice is similar to that in NdCo$_2$ above T_M and to that in TbCo$_2$ below T_M, respectively. The mixing of Nd and Tb in (Nd$_{0.5}$Tb$_{0.5}$)Co$_2$ reduces both the R sublattice anisotropy and the difference of sublattice magnetization $|M_R - M_{Co}|$, which are responsible for the observations in this work. The mixed compounds (R', R'')Co$_2$ between light and heavy rare earths with different anisotropic characters are ideal systems for enhancing our understanding of the physical properties of the RCo$_2$ Laves phases.

*Email address: ghrao@aphy.iphy.ac.cn

[1] K. A. Gschneidner, Jr., V. K. Pecharsky, and A. O. Tsokol, Rep. Prog. Phys. **68**, 1479 (2005).

[2] V. K. Pecharsky and K. A. Gschneidner, Jr., Phys. Rev. Lett. **78**, 4494 (1997).

[3] L. Morellon, J. Stankiewicz, B. García-Landa, P. A. Algarabel, and M. R. Ibarra, Appl. Phys. Lett. **73**, 3462 (1998).

[4] E. Gratz and A. S. Markosyan, J. Phys.: Condens. Matter **13**, R385 (2001).

[5] T. Goto, T. Sakakibara, K. Murata, H. Komatsu, and K. Fukamichi, J. Magn. Magn. Mater. **90&91**, 700 (1990).

[6] M. Cyrot and M. Lavagna, J. Phys. (Paris) **40**, 763 (1979).

[7] T. Moriya, J. Magn. Magn. Mater. **100**, 261 (1991).

[8] N. H. Due and P. E. Brommer, in *Handbook of Magnetic Materials*, edited by K. H. J. Buschow (North-Holland, Amsterdam, 1999), Vol. 12, p. 259.

[9] E. Gratz, A. Lindbaum, A. S. Markosyan, H. Mueller, and A. Yu Sokolov, J. Phys.: Condens. Matter **6**, 6699 (1994).

[10] J. R. Cullen and A. E. Clark, Phys. Rev. B **15**, 4510 (1977).

[11] P. E. Brommer, I. S. Dubenko, J. J. M. Franse, R. Z. Levitin, A. S. Markosyan, R. J. Radwanski, V. V. Snegirev, and A. V. Sokolov, Physica B **183**, 363 (1993).

[12] W. M. Swift and W. E. Wallace, J. Phys. Chem. Solids **29**, 2053 (1968).

[13] Z. W. Ouyang, G. H. Rao, H. F. Yang, W. F. Liu, and J. K. Liang, Appl. Phys. Lett. **81**, 97 (2002).

[14] Z. W. Ouyang, F. W. Wang, Q. Huang, W. F. Liu, Y. Q. Xiao, J. W. Lynn, J. K. Liang, and G. H. Rao, Phys. Rev. B **71**, 064405 (2005).

[15] Z. W. Ouyang, F. W. Wang, Q. Huang, W. F. Liu, G. Y. Liu, J. W. Lynn, J. K. Liang, and G. H. Rao, J. Alloys Compd. **390**, 21 (2005).

[16] H. M. Rietveld, Acta Crystallogr. **229**, 151 (1967).

[17] J. L. Rodríguez-Carvajal, Physica B **192**, 55 (1993).

[18] N. Baranov, E. Gratz, H. Nowotny, and W. Steiner, J. Magn. Magn. Mater. **37**, 206 (1983).

[19] A. V. Andreev, in *Handbook of Magnetic Materials*, edited by K. H. J. Buschow (Elsevier Science B. V., Amsterdam, 1995), Vol. 8, p. 61.

[20] Z. G. Zhao, X. Li, J. H. V. J. Brabers, P. F. de Châtel, F. R. de Boer, and K. H. J. Buschow, J. Magn. Magn. Mater. **123**, 74 (1993).